Bioinformatics and Functional Analysis of MicroRNAs that Regulate Expression of Human Fatty Acid Synthase Gene

การวิเคราะห์เชิงชีวสารสนเทศ และ ศึกษาการทำงานของ microRNA ที่ควบคุมการแสดงออกของยีน Fatty Acid Synthase

Tanapa Suksangrat (ธนาภา สุขแสงรัตน์)* Pannapa Pinweha (พรรณนภา ปิ่นเวหา)**

Dr.Sittinan Chanarat (ดร.สิทธินันท์ ชนะรัตน์)*** Dr.Sarawut Jitrapakdee (ดร.ศราวุฒิ จิตรภักดี)****

ABSTRACT

The human fatty acid synthase (hFASN) is one of key enzymes that regulate *de novo* fatty acid synthesis pathway and the upregulation of this gene is associated with non-alcoholic fatty liver disease and cancers. Herein, we use bioinformatics tools to identify several miRNAs that can potentially target expression of hFASN gene. These potential miRNAs include miR-27a, miR-27b, miR-495, miR-15a, miR-15b, miR-16, miR-195, miR-497, miR-424, miR-103 and miR-107. Transfection of reporter construct containing 3'-UTR of hFASN mRNA, placed downstream of luciferase reporter gene into HepG2 cells also down-regulates expression of luciferase activity by 50% but not in HEK293T cells, indicating the presence of functional miRNA binding sites. Truncations of both halves of the 3'-UTR of hFASN mRNA also affected the luciferase activity, suggesting that the miRNA binding sites are located on both halves of the 3'-UTR. To examine whether the above miRNAs were hepatocyte-specific, their expression profiles were also pulled out from miRmine, human miRNA expression databases.

บทคัดย่อ

เอนไซม์ fatty acid synthase (hFASN) เป็นเอนไซม์สำคัญที่ควบคุมกระบวนการสังเคราะห์กรดไขมัน และการแสดงออกที่เพิ่มขึ้นของยีนนี้เกี่ยวข้องกับภาวะตับแข็งและมะเร็งหลายชนิด งานวิจัยนี้ได้พิสูจน์หา microRNA (miRNA) ที่ควบคุมการแสดงออกของยีน *hFASN* โดยใช้การวิเคราะห์เชิงชีวสารสนเทศ พบว่า hFASN mRNA ถูกควบคุมด้วย miR-27a, miR-27b, miR-495, miR-15a, miR-15b, miR-16, miR-195, miR-497, miR-424, miR-103, miR-107 เมื่อทำการสร้างยีนลูกผสมโดยนำบริเวณ 3'-UTR ของ hFASN mRNA มาต่อหลังยีนลูซิเฟอเรส แล้วนำเข้าสู่เซลล์ HepG2 ส่งผลให้การแสดงออกของยีนลูซิเฟอเรสลดลง 50% และเมื่อแบ่ง 3'-UTR ของยีนนี้เป็นสองส่วน พบว่า miRNA จับกับ 3'-UTR ทั้งสองส่วน นอกจากนี้ฐานข้อมูล miRmine ยังยืนยันว่า miRNA ข้างต้นคือ miRNA ที่จำเพาะในเซลล์ตับ

Keywords: MicroRNA, NAFLD, Cancer

คำสำคัญ: ไมโครอาร์เอ็นเอ ภาวะตับแข็ง มะเร็ง

* *Student, Master of Science Program in Biochemistry, Faculty of Science, Mahidol University*

** *Student, Doctor of Philosophy Program in Biochemistry, Faculty of Science, Mahidol University*

*** *Lecturer, Department of Biochemistry, Faculty of Science, Mahidol University*

**** *Professor, Department of Biochemistry, Faculty of Science, Mahidol University*

Introduction

MicroRNAs (miRNAs) play important roles in post-transcriptional regulation of gene expression. They control various aspects of life including development, survival and metabolism. miRNAs are short double stranded RNAs, comprising 15-25 nucleotides (Bartel, 2004). Binding of miRNAs to their targets is mediated by hybridization of 7-8 nucleotides of the miRNAs (known as the 'seed match') to their complementary sequences in the 3'-untranslated region (3'-UTR) of mRNAs (Brennecke et al., 2005). Such hybridization results in degradation or translational inhibition of target mRNAs, thus providing a means to inhibit gene expression (Li, Rana, 2014). Aberrant expression of certain miRNAs is also associated with metabolic syndrome such as type 2 diabetes, non-alcoholic fatty liver disease (NAFLD) (Rottiers, Näär, 2012; Abente et al., 2016) or even in cancers (Hayes et al., 2014)

The *de novo* fatty acid synthesis is the synthesis of fatty acids from glucose. The fatty acid synthase (FASN) is one of key enzymes that regulates overall program of this pathway (Chirala et al., 2001). Aberrant expression of FASN is associated with non-alcoholic fatty liver disease (NAFLD) (Dorn et al., 2010; Neuschwander-Tetri, 2017). Up-regulation of FASN overexpression was also reported as one of metabolic reprogramming in several cancers in response to high demand of phospholipids during rapid proliferation (Jones, Infante, 2015).

Recently, several miRNAs that can be used as therapeutic drug have been reported. They act by down-regulating an aberrant expression of their target mRNAs (Rupaimoole, Slack, 2017). The identification of the miRNAs that target human FASN expression may provide a means to block hyperlipidemia in metabolic syndrome patients, and may also be an alternative strategy to block cancer growth. In this study, we used bioinformatics and functional studies to identify putative miRNAs that can regulate human FASN expression.

Objective of the study

To identify the microRNA(s) that regulates human FASN expression in hepatocytes.

Methodology

Bioinformatics identification of miRNA(s) that regulate human FASN

The prediction algorithms including miRANDA-miSVR (Betel et al., 2008; Betel et al., 2010), TargetScanHuman 7.1 (Agarwal et al., 2015) and miRDB web tools (Wong, Wang X, 2015; Wang X et al., 2016) were used to predict miRNA binding sites in the 3'-UTR of h*FASN* mRNA (NM_004104.4). These miRNA target prediction algorithms share some common features including seed match, sequence conservation across the species, free energy binding between miRNA and mRNA targets, and the site accessibility for scoring the candidate miRNA binding sites. The algorithms also show the alignments between the predicted miRNAs and 3'UTR of human FASN mRNA with scores of prediction and free energy binding, indicating the confidence of prediction.

Reporter plasmid constructs

To further confirm whether the human FASN is regulated by miRNA(s), the luciferase reporter vector, pmirGLO vector, containing 3'-UTR of human FASN cDNA wild type or truncated constructs (lacking nucleotides positions 1-406 and 407-782) were used in this research. The pmirGLO vector contains firefly luciferase gene (*luc*2)

driven by PGK promoter. The 3'-UTR of human FASN cDNA or its truncate mutants was inserted at *Sac*I and *Nhe*I restriction sites downstream of luciferase gene. To test this reporter system, pmirGLO containing miR-21 and mismatch miR-21 target sequences were used as positive and negative controls, respectively, in HEK293T cells because HEK293T cells express miR-21. These constructs were provided by Ms. Pannapa Pinweha. The miR-21 target and mismatch miR-21 target sequences were inserted between *Pme*I and *Xba*I restriction sites in pmirGLO reporter vector, and their sequences are shown in table 1. The pSV-β Galactosidase control vector (pSV-β-gal) encoding *lac* Z gene or β-galactosidase gene was used for normalizing the transfection efficiency by co-transfection with pmirGLO vector.

Table 1 miR-21 target and mismatch miR-21 target sequences (Underline indicates *Pme*I and *Xba*I restriction sites at their 5'-ends, used to facilitate cloning.)

Name	Sequence (5'→ 3')
miR-21 target	TTTAAACTAGCGGCCGCTAGTTCAACATCAGTCTGATAAGCTATCTAGA
Mismatch miR-21 target	TTTAAACTAGCGGCCGCTAGTTCAACATCAGAAGATAAGCTATCTAGA

Cell culture

To test whether predicted miRNA(s) is tissue-specific miRNA, HepG2 cells (as a representative of hepatocyte) and HEK293T cells (as a non-hepatocyte) were used in this study. HepG2 (HB-8065™) and HEK293T (CRL-3216™) were cultured in Dulbecco's Modified Eagle high glucose medium (DMEM) containing 10% (v/v) heat-inactivated fetal bovine serum (FBS) and 1% (v/v) penicillin/streptomycin and incubated at 37°C in 5% CO_2 incubator. For transfection experiment, these cells were cultured in DMEM containing 10% FBS without antibiotics before transfection.

Transient transfections

1×10^5 HepG2 cells or HEK293T cells were seeded in 24-wells plate containing 500 µl of DMEM medium supplemented with 10% (v/v) FBS without antibiotics for 24 h. On the transfection day, two cocktail reagents were prepared. First cocktail contained 2 µl of LipofectAMINE™ 2000 reagent in 50 µl of OptiMEM® I while second cocktail contained 0.07 pmol of luciferase reporter construct and 250 ng of pSV-β-gal plasmid in 50 µl of OptiMEM® I. Both cocktails were gently mixed before incubated at room temperature for 5 min. The culture medium was replaced by 400 µl of fresh medium before transfection with 100 µl transfection mixture and the cells were incubated at 37°C for 48 h in CO_2 incubator.

Luciferase reporter assay

After 48 h. transfection, transfected cells were washed with 1× PBS solution pH 7.4 and lysed in 100 µl of 1x cell culture lysis reagent buffer (Promega) followed by transferring to new centrifuged tube and storing at -80°c. The lysate was centrifuged at 13,000×g at 4°C for 10 min after 2 cycles of freeze/thaw process. Finally, the supernatant was collected, and protein concentrations were measured by Bradford assay (Bradford, 1976).

One hundred microliters reaction mixture containing 20 mM Tris-phosphate pH 7.8, 4.07 mM $MgCl_2$, 2.7 mM $MgSO_4$, 33.3 mM DTT, 0.1 mM EDTA, 0.27 mM acetyl CoA, 0.53 mM ATP pH 7.8 and 0.47 mM beetle luciferin was subjected into 20-50 µg of protein samples by luminometer (Glomax®20/20, Promega) and the luciferase activity was calculated by following equation.

$$\text{Enzyme activity} = \frac{\text{light intensity unit}}{\text{protein amount } (\mu g)}$$

**The enzyme activity was normalized with β-galactosidase activity.

The pSV-β-gal plasmid was used as a normalizer to minimize the variation of transfection efficiency between the experiments. This pSV-β-gal plasmid was co-transfected with pmirGLO containing 3'UTR of human *FASN* wild type cDNA and its mutant constructs. The *lac Z* gene in pSV-β-gal plasmid was encoded for β-galactosidase enzyme which catalyzes the hydrolysis of *o*-p-nitrophenyl-β-D-galactopyranoside (ONPG), substrate, to yellow product, *o*-nitrophenol.

Two hundreds and fifty microliters of reaction buffer containing 100 mM sodium phosphate buffer pH 7.3, 1 mM $MgCl_2$, 10 mM KCl, 50 mM β-mercaptoethanol was mixed with 20-50 µg of protein samples before incubated at 37°C for 10 min. Fifty microliters of 2 mg/ml ONPG were added to reaction mixture and were then incubated with shaking until solution turns to yellow. After that, 100 µl of yellow product were mixed with 100 µl of 1 M Tris-HCl pH 8.0 in 96-well plate to stop the reaction. The absorbance at 414 nm of yellow product was measured by microplate reader (Thermo Labsystems) and β-galactosidase activity was calculated using following equation.

$$\beta\text{-galactosidase activity} = \frac{(\text{OD414 transfected cell - OD414 untransfected cell}) \times 100}{\text{Protein amount } (\mu g) \times \text{incubation time (hours)}}$$

Statistical analysis

The quantitative data are shown as the mean ± S.D. The statistical analysis was performed using one way analysis of variance (one-way ANOVA) followed by Student-Newman-Keuls test using SigmaStat® version 3.5 (Systat Software, Inc., California)

Results

To examine whether human FASN is regulated by miRNAs, its 3'-UTR mRNA was analyzed by various web tools i.e., miRanda-mirSVR (Betel et al., 2008; Betel et al., 2010), TargetScanHuman 7.1 (Agarwal et al., 2015) and miRDB web tools (Wong, Wang, 2015; Wang et al., 2016). Eleven predicted miRNAs with relatively high score, namely miR-27a, miR-27b, miR-495, miR-15a, miR-15b, miR-16, miR-195, miR-497, miR-424, miR-107, miR-103a were shown in Venn diagram (Figure 1A) and their binding sites were identified in 3'-UTR of human *FASN* cDNA (Figure 1b). miR-27a and miR-27b shared the same seed sequences and located between nucleotides 227 and 233 (named as position 1) in the 3'UTR of human FASN cDNA. miR-495 had a seed sequence located between nucleotides 652 and 659 (named as position 2) in the 3'UTR of human FASN cDNA. miR-15a, miR-15b, miR-16, miR-195, miR-497, miR-424 which are classified as miR-15 family shared the same seed sequences and located

between nucleotides 680 and 686 (named as position 3) and miR-15 family including miR-107, miR-103a family shared the same seed sequences located between nucleotides 763 and 769 (named as position 4) in 3'UTR of human FASN cDNA. The TargetScanHuman 7.1 web tools showed that predicted miRNA binding sites positions 1 and 3 were highly conserved across species (Figure 2A) and with their scores, high minus scores (context++ score) mean high probability of being true targets (Figure 2B).

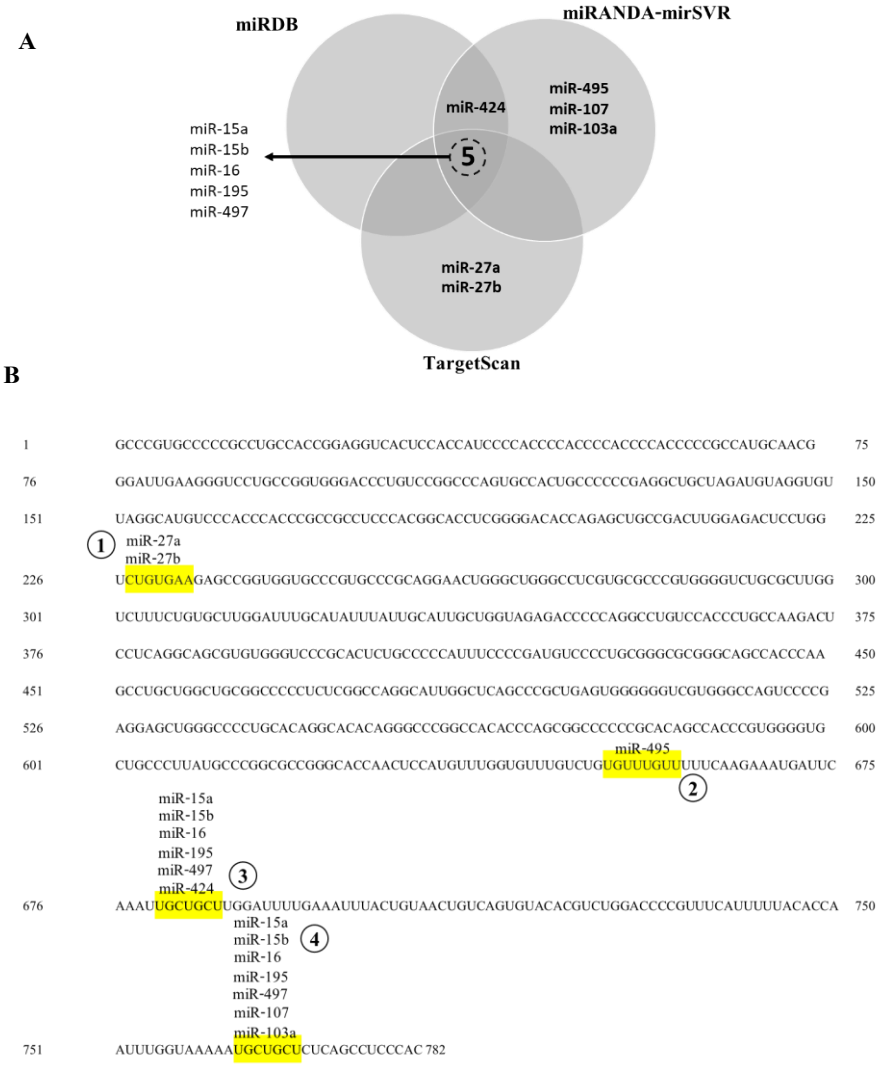

Figure 1 (A) Venn diagram showing eleven predicted miRNAs namely, miR-27a, miR-27b, miR-495, miR-15a, miR-15b, miR-16, miR-195, miR-497, miR-424, miR-107, miR-103a. (B) The 3'UTR of human *FASN* (NM_004104.4) and all predicted miRNA binding sites from various web tools.

A

```
                5'-...227....233.....................680...686........-3' FASN mRNA
Human       --GGUCUGUGA----AGAGCCGGUG--......-AAUUGCUGCUU-GGAUUUU
Chimp       --GGUCUGUGA----AGAGCCGGUG--......-AAUUGCUGCUU-GGAUUUU
Rhesus      --GGUCUGUGA----AGAGCCGGCG--......-AAUUGCUGCUC-GGGUUUU
Squirrel    --GAUCUGUGA----AGAGCCAGCG--......-GAUGGCUGCUG-GGGUUUU
Mouse       --GGUCUGUGA----AGAGUCAGUG--......-AAU-GAUGCUU-GGGUUUU
Rat         --GGUCUGUGA----AGAGUCAGUG--......-AAUUGCUGCUU-GGGUUUU
```

B

	Predicted consequential pairing of target region (top) and miRNA (bottom)	Site type	Context++ score	Context++ score percentile	Weighted context++ score	Conserved branch length	PCT
Position 227-233 of FASN 3' UTR hsa-miR-27b-3p	5' ...UUGGAGACUCCUGGUCUGUGAAG... 3' CGUCUUGAAUCGGUGACACUU	7mer-A1	-0.04	62	-0.04	5.716	0.71
Position 227-233 of FASN 3' UTR hsa-miR-27a-3p	5' ...UUGGAGACUCCUGGUCUGUGAAG... 3' CGCCUUGAAUCGGUGACACUU	7mer-A1	-0.04	62	-0.04	5.716	0.71

	Predicted consequential pairing of target region (top) and miRNA (bottom)	Site type	Context++ score	Context++ score percentile	Weighted context++ score	Conserved branch length	PCT
Position 680-686 of FASN 3' UTR hsa-miR-195-5p	5' ...AGAAAUGAUUCAAAUUGCUGCUU... 3' CGGUUAUAAAGAC-ACGACGAU	7mer-m8	-0.31	95	-0.31	4.691	0.69
Position 680-686 of FASN 3' UTR hsa-miR-16-5p	5' ...AGAAAUGAUUCAAAUUGCUGCUU... 3' GCGGUUAUAAAUGC-ACGACGAU	7mer-m8	-0.31	95	-0.31	4.691	0.69
Position 680-686 of FASN 3' UTR hsa-miR-15a-5p	5' ...AGAAAUGAUUCAAAUUGCUGCUU... 3' GUGUUUGGUAAUACACGACGAU	7mer-m8	-0.29	95	-0.29	4.691	0.69
Position 680-686 of FASN 3' UTR hsa-miR-424-5p	5' ...AGAAAUGAUUCAAAUUGCUGCUU... 3' AAGUUUUGUACUUAACGACGAC	7mer-m8	-0.27	94	-0.27	4.691	0.69
Position 680-686 of FASN 3' UTR hsa-miR-497-5p	5' ...AGAAAUGAUUCAAAUUGCUGCUU... 3' UGUUUGGUGUCACACGACGAC	7mer-m8	-0.27	94	-0.27	4.691	0.69
Position 680-686 of FASN 3' UTR hsa-miR-15b-5p	5' ...AGAAAUGAUUCAAAUUGCUGCUU... 3' ACAUUUGGUACUACACGACGAU	7mer-m8	-0.28	94	-0.28	4.691	0.69

Figure 2 (A) Sequence alignment of two predicted miRNA binding sites (nucleotides 227-233) in 3' UTR of FASN mRNAs of human, chimpanzee, rhesus macaque, squirrel, mouse, and rat and (B) predicted miRNA with their scores, high minus scores (context++ score) mean high probability of being true targets (Agarwal et al., 2015).

To further confirm that predicted miRNAs can regulate human FASN, the luciferase reporter assay was performed using pmirGLO reporter containing 3'UTR of human FASN cDNA (wild type) or its truncated mutants (lacking nucleotide positions 1-406 and 407-782) was co-transfected with pSV-β-gal plasmid into HepG2 cells. Placing 3'-UTR of human FASN cDNA downstream of the luciferase reporter gene lowered luciferase reporter activity by 50% compared with pmirGLO empty vector ($p < 0.001$) (Figure 3A). Furthermore, truncation of 3'UTR of human FASN cDNA, lacking nucleotides between 1-406 or 407-782 also resulted in 30% and 25% reduction of luciferase reporter activity ($p < 0.01$), respectively. As a positive control of the pmirGLO reporter system, transfection of pmirGLO reporter plasmid containing miR-21 target sequence into HEK293T cells (non-hepatocytes) resulted in 40% reduction of luciferase activity, compared with the mismatch miR-21 target and pmirGLO empty vector ($p < 0.05$) (Figure 3B). This result demonstrated that the reporter system worked properly. On the other hand, the transfection of pmirGLO containing 3'UTR of human FASN cDNA wild type and truncate mutants into non-hepatocytes, HEK293T cells, did not affect luciferase activity compared with pmirGLO empty vector (Figure 2B).

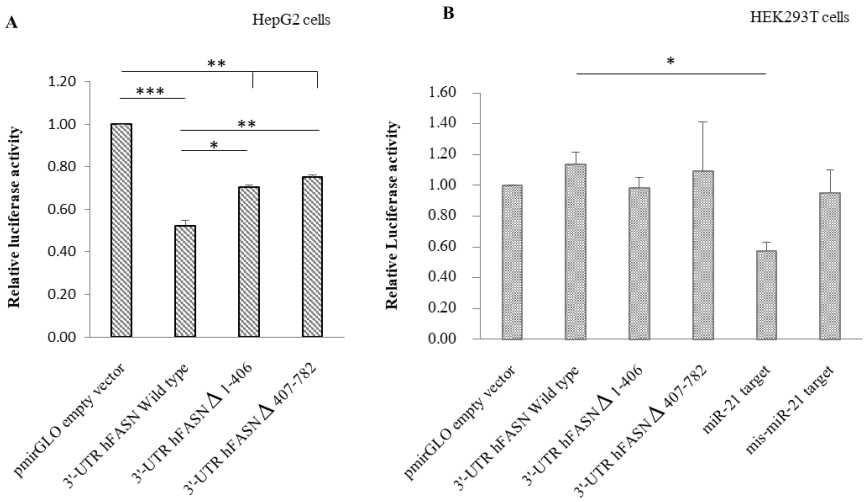

Figure 3 The relative luciferase activity detected in HepG2 cell (A) transfected with pmirGLO constructs (empty vector), pmirGLO containing 3'UTR of human FASN cDNA wild type, truncate mutants lacking nucleotides positions 1-406 and 407-782. The relative luciferase activity of HEK293Tcell (B) transfected with the same constructs and pmirGLO containing miR-21 target sequence and mismatch miR-21 target sequence as a positive and negative control, respectively. The luciferase activity is relatively calculated to pmirGLO empty vector which was set as 100%. The results are shown as means ± S.D. of two independent experiments, each in duplicate. *p < 0.05, **p < 0.01, ***P < 0.001

To confirm the existence of these predicted miRNAs, their expression profiles in various cell lines including HepG2 cells, HEK293T cells (non-hepatocyte), MCF-7 (breast cancer) were explored from miRmine, human miRNA expression databases (Panwar et al., 2017). The expression profiles showed that all of predicted miRNAs were expressed in various cell lines except miR-495 (Figure 4).

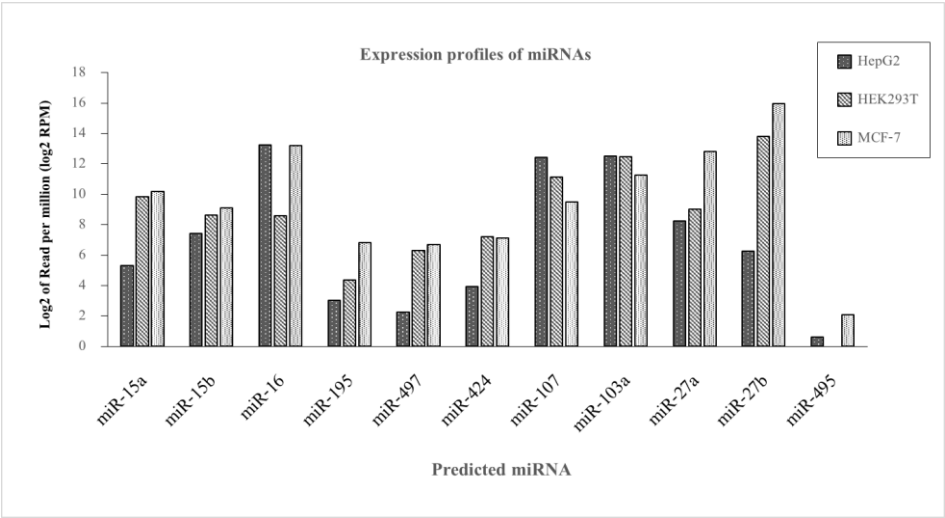

Figure 4 Expression profiles of predicted miRNAs in HepG2, HEK293T (non-hepatocytes) and MCF-7 (breast cancer) cells. Unit of expression values shows in Log2 of read per million (log2 RPM) (Panwar et al., 2017).

Discussion and Conclusion

TargetScanHuman 7.1 web tool (Agarwal et al., 2015) predicts the miRNA binding sites based on seed match and conservation across species features, suggesting that this analysis provides evidence that the predicted miRNA binding sites are functional (Peterson et al., 2014). Therefore, it is likely that predicted miR-27a, miR-27b (target positions 1 in 3'-UTR of human FASN) and miR-15 family (target positions 2 in 3'-UTR of human FASN) would regulate FASN expression. Moreover, miRANDA-mirSVR (Betel et al., 2008; Betel et al., 2010) and miRDB (Wong, Wang, 2015; Wang et al., 2016) web tools also share the same common features in prediction and include free energy and site accessibility. The free energy is used to indicate miRNA:mRNA target interaction stability. The site accessibility provides the information regarding the ease of miRNAs access to their target sites (Peterson et al., 2014). For expression of miRNAs results, although miR-495 showed low expression in various cell lines, the expression of miR-495 will be evaluated further.

The 50% reduction of relative luciferase activity from 3'-UTR of human FASN wild type in HepG2 cells indicates that 3'UTR of human FASN mRNA mediates its inhibitory effect on expression of luciferase reporter gene. While inhibitory effect of the 3'-UTR on luciferase expression is apparent in HepG2 cells, this was not the case for HEK293T cells. This clearly indicates that the regulation of human FASN by miRNAs is hepatocyte-specific. Furthermore, truncations of the 5'- or 3'-half of human FASN UTR also resulted in 30% and 25% reduction of luciferase activity, suggesting that the repressive element(s) which confer miRNA regulation is located at both halves of 3'-UTR of human FASN mRNA. These results are consistent with the prediction algorithm results which show the presence of eleven miRNA binding sites and four of which are located at both halves of 3'-UTR of human FASN mRNA. There are some investigators reported involvement of certain miRNAs in regulation of FASN in certain cancers such as miR-15a, miR-16, miR-195 in breast cancer (Singh et al., 2015; Wang J et al., 2016), miR-195, miR-424 in osteosarcoma cell (Mao et al.,2012; Long et al., 2013). Nevertheless, neither of them studied expression in hepatocytes.

In conclusion, eleven miRNAs, namely miR-27a, miR-27b, miR-495, miR-15a, miR-15b, miR-16, miR-195, miR-497, miR-424, miR-107, miR-103a were identified to target at their four binding sites in 3'-UTR of human FASN mRNA. To further confirm which miRNAs regulate human FASN, the expression of miRNA(s) in HepG2 cells will be measured and the luciferase assay should be performed with mutations of their four binding sites in 3'-UTR of human FASN construct. Moreover, the effect of these miRNAs on endogenous human FASN should also be further studied.

Acknowledgements

This study was supported by the Thailand Research Fund, grant BRG 6080005.

References

Abente E.J., Subramanian M, Ramachandran V, Najafi-Shoushtari S.H. MicroRNAs in obesity-associated disorders. Archives of Biochemistry and Biophysics 2016; 589: 108-119

Agarwal V, Bell GW, Nam J-W, Bartel DP. Predicting effective microRNA target sites in mammalian mRNAs. Izaurralde E, ed. *eLife*. 2015; 4: e05005.

Bartel D.P. MicroRNAs. Cell 2004; 116(2): 281-297.

Bradford M.M. Rapid and sensitive method for the quantitation of microgram quantities of protein utilizing the principle of protein-dye binding. Analytical Biochemistry 1986; 72: 248–254

Brennecke J, Stark A, Russell R.B., Cohen, S.M. Principles of MicroRNA–Target Recognition. PLOS Biology 2005; 3(3): e85.

Betel D, Wilson M, Gabow A, Marks D.S, Sander C. The microRNA.org resource: targets and expression. Nucleic Acids Research 2008; 36: D149-D153.

Betel D, Koppal A, Agius P, Sander C, Leslie C. Comprehensive modeling of microRNA targets predicts functional non-conserved and non-canonical sites. Genome Biology 2010; 11(8): R90.

Chirala S.S, Jayakumar A, Gu Z.-W, Wakil S.J. Human fatty acid synthase: Role of interdomain in the formation of catalytically active synthase dimer. Proceedings of the National Academy of Sciences of the United States of America 2001; 98(6): 3104-3108.

Dorn C, Riener M.-O, Kirovski G, Saugspier M, Steib K, Weiss T.S. Expression of fatty acid synthase in nonalcoholic fatty liver disease. Int J Clin Exp Pathol 2010; 3(5): 505-514.

Hayes J, Peruzzi P.P, Lawler S. MicroRNAs in cancer: biomarkers, functions and therapy. Trends in Molecular Medicine 2014; 20(8): 460-469.

Jones S.F, Infante J.R. Molecular Pathways: Fatty Acid Synthase. Clinical Cancer Research 2015; 21(24): 5434-5438.

Li Z, Rana, T.M. Therapeutic targeting of microRNAs: current status and future challenges. Nature Reviews Drug Discovery 2014; 13(8): 622-638.

Long X.H, Mao J.H, Peng, A.F. Tumor suppressive microRNA-424 inhibits osteosarcoma cell migration and invasion via targeting fatty acid synthase. Experimental and Therapeutic Medicine 2013; 5(4): 1048-1052.

Mao J.H, Zhou R.P, Peng A.F. microRNA-195 suppresses osteosarcoma cell invasion and migration in vitro by targeting FASN. Oncology Letters 2012; 4(5): 1125-1129.

Mashima T, Seimiya H, Tsuruo T. De novo fatty-acid synthesis and related pathways as molecular targets for cancer therapy. British Journal of Cancer 2009; 100(9): 1369-1372.

Neuschwander-Tetri B.A. Non-alcoholic fatty liver disease. BMC Medicine 2017; 15(1): 45.

Panwar B, Omenn GS, Guan Y. miRmine: A Database of Human miRNA Expression Profiles. Bioinformatics 2017 [online] 2017 [cited 2017 Dec 31]. Available from: http://guanlab.ccmb.med.umich.edu/mirmine

Peterson S, Thompson J, Ufkin M, Sathyanarayana P, Liaw L, Congdon C.B. Common features of microRNA target prediction tools. Frontiers in Genetics 2014; 5(23).

Rottiers V, Näär A.M. MicroRNAs in metabolism and metabolic disorders. Nature Reviews Molecular Cell Biology 2012; 13(4): 239-250.

Rupaimoole R, Slack F.J. MicroRNA therapeutics: towards a new era for the management of cancer and other diseases. Nature Reviews Drug Discovery 2017; 16(3): 203-222.

Singh R, Yadav V, kumar S, Saini N. MicroRNA-195 inhibits proliferation, invasion and metastasis in breast cancer cells by targeting FASN, HMGCR, ACACA and CYP27B1. Sci Rep 2015; 5.

Wang J, Zhang X, Shi J, Cao P, Wan M, Zhang Q et al. Fatty acid synthase is a primary target of MiR-15a and MiR-16-1 in breast cancer. Oncotarget 2016; 7(48): 78566-78576.

Wang X. Improving microRNA target prediction by modeling with unambiguously identified microRNA-target pairs from CLIP-ligation studies. Bioinformatics 2016; 32(9): 1316-1322.

Wong N, Wang X. miRDB: an online resource for microRNA target prediction and functional annotations. Nucleic Acids Research 2015; 43(D1): D146-D152.